ORIGINAL ARTICLE

Targeting Diabetes Pathways: An *in silico* Study of Bioactive Compounds from *Mitragyna speciosa* Leaf Extract

Taslima Begum[1], Qamar Uddin Ahmed[1*], Mohd Hafiz Arzmi[2], Syed Adnan Ali Shah[3], Mohd Salleh Rofiee[4], Murni Nazira Sarian[5], ABM Helal Uddin[1], Muhammad Muzaffar Ali Khan Khattak[6]

[1]Drug Discovery and Synthetic Chemistry Research Group, Department of Pharmaceutical Chemistry, Kulliyyah of Pharmacy, International Islamic University Malaysia (IIUM), 25200 Kuantan, Pahang Darul Makmur, Malaysia; taslimabegum790@gmail.com (T.B.), quahmed@iium.edu.my (Q.U.A), abmhelal@iium.edu.my (A.B.M.H.U.)

[2]Department of Fundamental Dental and Medical Sciences, Kulliyyah of Dentistry, International Islamic University Malaysia, 25200 Kuantan, Pahang, Malaysia; hafizarzmi@iium.edu.my (M.H.A.)

[3]Faculty of Pharmacy, Atta-ur-Rahman Institute for Natural Products Discovery (AuRIns), Universiti Teknologi MARA, Cawangan Selangor Kampus Puncak Alam, 42300 Bandar Puncak Alam, Selangor, Malaysia; syedadnan@uitm.edu.my (S.A.S.)

[4]Integrative Pharmacogenomics Institute (iPROMISE), Universiti Teknologi MARA, Cawangan Selangor Kampus Puncak Alam, 42300 Bandar Puncak Alam, Selangor, Malaysia; sallehrofiee@uitm.edu.my (M.S.R.)

[5]Institute of Systems Biology (INBIOSIS), Universiti Kebangsaan Malaysia, 43600, Bangi, Selangor, Malaysia; murninazira@ukm.edu.my (M.N.S.)

[6]Food Security and Public Health Nutrition Research Group (Foster), Department of Nutrition Sciences, Kulliyyah of Allied Health Sciences, IIUM, 25200 Kuantan, Pahang Darul Makmur, Malaysia

ABSTRACT

Background: The rapid expansion of urbanization has triggered significant lifestyle shifts, most notably an increase in sedentary lifestyles and the widespread consumption of processed, nutrient-poor foods. These factors have been strongly implicated in the rising prevalence of Diabetes Mellitus. Current treatment strategies for diabetes remain heavily reliant on conventional pharmacotherapy, which often carries risks of drug tolerance and adverse effects. In this context, Kratom (*Mitragyna speciosa*), a traditional medicinal plant native to Southeast Asia and historically used to manage various ailments, presents a promising avenue for the development of novel antidiabetic agents. **Methods:** In this study, kratom leaf extract was prepared using methanol-based maceration of kratom leaf powder to obtain a 100% methanolic extract (100%M). The extract was subsequently analyzed using Q-Tof-LCMS, leading to the putative identification of bioactive compounds. These compounds were further subjected to molecular docking against two key target proteins, namely PDB codes 3A4A and 4N8D, to assess their binding affinities. **Results:** The results revealed several promising candidates including apigenin 7-(2''-*E*-*p*-coumaroylglucoside, kaempferol 3-(2''-(*Z*)-*p*-coumaryl-6''-(*E*)-*p*-coumarylglucoside, 5,6,7,3',4'-pentahydroxy-8-methoxyflavone 7-apioside, luteolin 7-rhamnosyl(1->6)galactoside and 6-hydroxyluteoin-7-(6'''-*p*-coumarylsophoroside), all of which demonstrated stronger binding affinities than both the standard and native ligands. Further evaluation of physicochemical and pharmacokinetic parameters revealed that 4-*p*-coumaroylquinic acid, scopolin, and emmotin A showed instant drug likeness, indicating their potential for direct drug development. Additionally, other compounds with high binding energies may be optimized through structural modifications to enhance their pharmacological profiles, thereby serving as lead candidates for the development of novel antidiabetic therapeutics. **Conclusion:** The current study has identified promising lead compounds for the development of novel antidiabetic agents, offering valuable guidance for future research on kratom-based antidiabetic drug discovery.

Keywords:
Diabetes, kratom, leaf, PDB, maceration, antidiabetic, drug likeness.

INTRODUCTION

Diabetes is a chronic health condition that arises when the body is unable to produce sufficient insulin or cannot effectively utilize the insulin it produces, leading to elevated blood glucose levels (hyperglycaemia).

It is recognized as one of the fastest-growing global health challenges of the 21st century. In 2024, an estimated 589 million people aged 20-79 were living with diabetes worldwide. This number is projected to increase by 45%, reaching nearly 853 million by 2050. In Southeast Asian countries such as Malaysia, Indonesia, the Philippines, and Thailand, the incidence of diabetes is expected to rise by as much as 73% according to the

Corresponding author.
E-mail address: muzaffar@iium.edu.my, quahmed@iium.edu.my

International Diabetes Federation report (2025). These alarming trends highlight the urgent need for effective strategies in prevention, management, and treatment.

Among the different types of diabetes, type 2 diabetes accounts for the majority of cases worldwide (>90%). Although it can often be prevented, delayed, or even reversed in its early stages (International Diabetes Federation report, 2025), it remains a major global health concern. In addition to lifestyle modifications such as adopting a more active routine and healthier dietary choices, treatment with appropriate antidiabetic drugs is also essential. However, conventional synthetic antidiabetic drugs are frequently associated with tolerance, resistance, and adverse side effects (Pollack et al., 2010). This underscores the urgent need to develop novel antidiabetic agents derived from natural sources, particularly traditional medicinal plants, which have long been used by communities to manage various health conditions.

In Southeast Asia, among the diverse range of medicinal plants, kratom (*Mitragyna speciosa*) (Figure 1) stands out as one of the most prominent species with potential for the development of novel antidiabetic agents, owing to its long history of traditional uses (Begum et al., 2025a). Thus, a range of scientific studies have been performed to investigate the antidiabetic properties of kratom leaf using *in vitro*, *in vivo*, and *in silico* models. For instance, Limcharoen et al. (2022) reported the *in vitro* α-glucosidase inhibitory activity of three different kratom extracts, as well as its major alkaloid, mitragynine. Similarly, Zhang et al. (2023) investigated the antidiabetic potential of kratom ethanol extract through both in vitro α-glucosidase inhibition assays and *in vivo* studies in a rat model, further supporting its therapeutic promise.

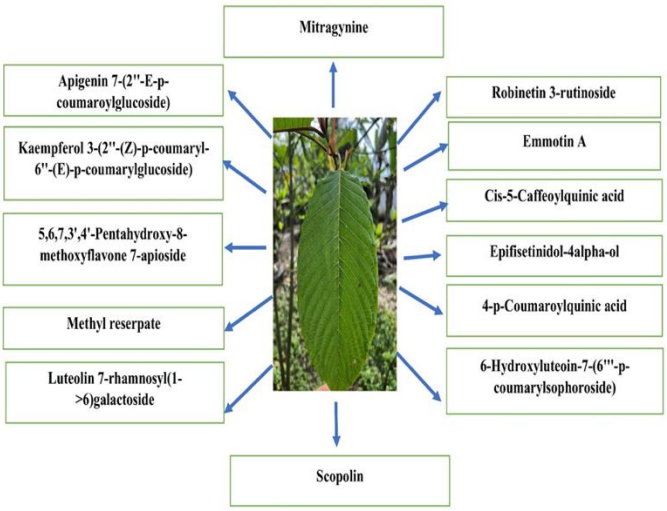

Figure 1: Kratom leaf along with the identified compounds

Furthermore, Hossain et al. (2023) demonstrated the antidiabetic properties of kratom leaves collected from Rangamati, Bangladesh, using both *in vivo* (Swiss albino mice) and *in silico* models (PDB ID: 5T4H). In addition, a clinical study conducted in West Kalimantan, Indonesia, evaluated the blood glucose response to kratom tea in ten participants. The study design involved three phases: administration of standard glucose in the 1st week, followed by administration of standard glucose combined with 1% kratom tea in the 2nd week, and a one-week washout period without treatment. The outcomes exhibited that kratom tea exhibited potential in reducing blood glucose levels (Fadly, 2025).

The objective of this article was to prepare a kratom leaf extract and identify its phytochemical constituents through Q-ToF-LCMS. The identified compounds were subsequently subjected to molecular docking analysis against two key antidiabetic targets: the α-glucosidase enzyme (PDB code: 3A4A) and dipeptidyl peptidase-4 (DPP-4) (PDB code: 4N8D). Finally, physicochemical and pharmacokinetic parameters of the docked compounds were evaluated to assess their potential as lead candidates for the development of novel antidiabetic therapeutics.

MATERIALS AND METHODS

Plant Material Collection and Identification

Kratom leaves were collected from Kedah, Malaysia and taxonomically verified at the Kulliyyah of Pharmacy, International Islamic University Malaysia (voucher no. PIIUM 0358). The leaves were completely cleaned with water to eliminate adhering soil and debris. Later, the cleaned leaves were carefully dried at 40 °C for 72 hours. After that, the dried material was pulverized into a coarse powder using a Universal cutting mill, yielding the powdered kratom leaf material for further analysis.

Extraction Through Maceration

A total of 100 g of dried kratom leaf powder was macerated in 100% methanol at a ratio of 1:3 (w/v) for 24 hours. The mixture was filtered, and the resulting filtrate was concentrated using a rotary evaporator at 40 °C. The recovered methanol was reintroduced to the plant residue, and the extraction process was repeated twice under the same conditions. In total, the procedure was performed three times to obtain 100% methanol maceration extract (100%M) (Begum et al., 2025b).

Profiling of Bioactive Compounds in *M. speciosa* leaf 100%M via Quadrupole Time-of-Flight Liquid Chromatography Mass Spectrometry (Q-ToF-LCMS)

Bioactive compound profiling was performed by employing the Agilent 1290 Infinity and 6550 iFunnel Q-ToF-LCMS (Agilent Technology, Santa Clara, CA, USA) equipped with an electrospray ionization (ESI) source operating in both +ve and -ve ionization modes. For sample preparation, 1 mg of the 100%M extract was allowed to dissolve in 250 µL of LC-grade methanol, followed by vortexing and ultrasonication. Subsequently, 250 µL of distilled water was added, yielding a final volume of 500 µL. The solution was allowed to centrifuge for fifteen minutes and filtered to get a clear solution. Later, it was transferred into a vial for analysis. Chromatographic separation was carried out on a Phenomenex Kinetex C18 column (250 mm × 4.6 mm, 5 µm) maintained at 27°C. The mobile phase consisted of methanol and 0.1% formic acid, with a gradient elution starting at 5% methanol and increasing to 100% methanol. The total run time was 10 minutes with a flow rate of 0.7 mL/min. Mass spectrometric data were acquired in the m/z range of 50 to 1500 with a collision energy ramp of 35 eV. Source parameters were maintained as follows: gas temperature 200 °C, flow rate 14 L/min, nebulizer pressure 35 psig, sheath gas temperature 350 °C, and sheath gas flow 11 L/min. The acquired data were processed using ACD/Spec Manager and pre-processed with MZmine software, including baseline correction, peak detection, filtering, alignment, smoothing, and gap filling. The processed data were exported in CSV format for further analysis (Ananda et al., 2025).

***In silico* Molecular Docking Analysis**

Molecular docking was done to determine the predicted binding affinities of the identified bioactive phytoconstituents at the active sites of the α-glucosidase enzyme (PDB code: 3A4A) and DPP-4 (PDB code: 4N8D) (https://www.rcsb.org/). The three-dimensional (3D) structures of the positive controls, i.e., acarbose for α-glucosidase and sitagliptin for DPP-4, as well as the identified compounds from Q-ToF-LCMS analysis, were retrieved from the PubChem database (https://pubchem.ncbi.nlm.nih.gov/). Docking was performed using AutoDock Vina, Autodock Tools 1.5.7, and Discovery Studio (Trott & Olson, 2010). For α-glucosidase (3A4A), redocking of the native ligand was conducted with grid dimensions (X, Y, Z) set to 26, 26, and 26, respectively, and grid center coordinates (X, Y, Z) set to 21.243, -7.756, and 24.341. For DPP-4 (4N8D), the grid dimensions were set to 26.0, 24.0, and 26.0, respectively, with grid center coordinates (X, Y, Z) of 18.3, 30.424, and 53.897, which were used for redocking of the native ligand. These docking setups ensured that the RMSD values of the redocked native ligands were less than 2 Å, confirming the reliability of the docking protocol. The binding interactions between the proteins and the docked compounds were subsequently analyzed in both two-dimensional (2D) and three-dimensional (3D) representations using Discovery Studio (Mia et al., 2022).

Physico-Chemical and Pharmacokinetic Properties

To predict a drug's behaviour in the body, optimize its therapeutic efficacy, and ensure safety, it is essential to evaluate its physicochemical and pharmacokinetic parameters. Hence, the bioactive compounds identified from the 100%M extract by Q-ToF-LCMS analysis were also investigated for their physicochemical and pharmacokinetic parameters. This evaluation was performed to forecast their drug-likeness and ADMET (Absorption, Distribution, Metabolism, Excretion, and Toxicity) profiles, thereby providing insights into their potential as lead candidates for antidiabetic drug development (http://www.swissadme.ch/index.php, https://biosig.lab.uq.edu.au/pkcsm/prediction) (Ananda et al., 2025).

RESULTS

% Yield and Q-ToF-LCMS Analysis of *M. speciosa* leaf 100%M Extract

The 100%M extract (yield: 30.17 %) was found to contain a diverse range of phytochemical constituents, as identified through Q-ToF-LCMS analysis in both positive and negative ionization modes (Table 1). The representative chromatograms obtained from each ionization mode are presented in Figure 2, while the chemical structures of selected identified phytoconstituents are illustrated in Figure 3.

Table 1: Identified compounds of *M. speciosa* leaf 100%M extract

Identified compounds	RT	Score	Formula	m/z
cis-5-Caffeoylquinic acid	7.43	95.67	$C_{16}H_{18}O_9$	353
Scopolin	7.44	99.58	$C_{16}H_{18}O_9$	355
Apigenin 7-(2''-*E*-*p*-coumaroylglucoside)	7.88	97.7	$C_{30}H_{26}O_{12}$	577
4-*p*-Coumaroylquinic acid	8.11	99.75	$C_{16}H_{18}O_8$	337
Epifisetinidol-4alpha-ol	8.12	98.73	$C_{15}H_{14}O_6$	289
Robinetin 3-rutinoside	8.77	95.09	$C_{27}H_{30}O_{16}$	609
Kaempferol 3-(2''-(*Z*)-*p*-coumaryl-6''-(*E*)-*p*-coumarylglucoside)	8.80	98.64	$C_{39}H_{32}O_{15}$	739
5,6,7,3',4'-Pentahydroxy-8-methoxyflavone 7-apioside	8.98	96.62	$C_{21}H_{20}O_{12}$	463
Luteolin 7-rhamnosyl(1->6)galactoside	8.99	99.07	$C_{27}H_{30}O_{15}$	593
6-Hydroxyluteoin-7-(6'''-*p*-coumarylsophoroside)	9.73	99.52	$C_{36}H_{36}O_{19}$	771
Methyl reserpate	10.18	99.25	$C_{23}H_{30}N_2O_5$	415
Mitragynine	11.07	99.6	$C_{23}H_{30}N_2O_4$	399
Emmotin A	16.95	94.76	$C_{16}H_{22}O_4$	279

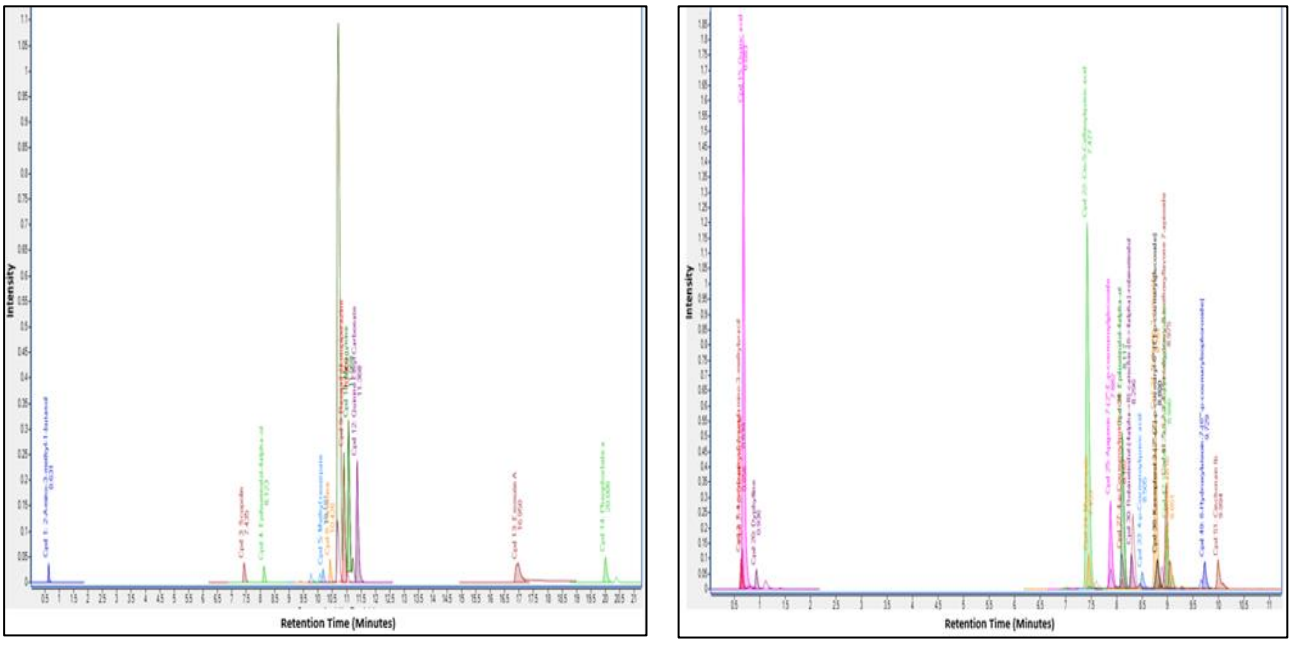

A B

Figure 2: Q-ToF-LCMS chromatograms of both positive (A) and negative (B) ionization modes of *M. speciosa* leaf 100%M extract

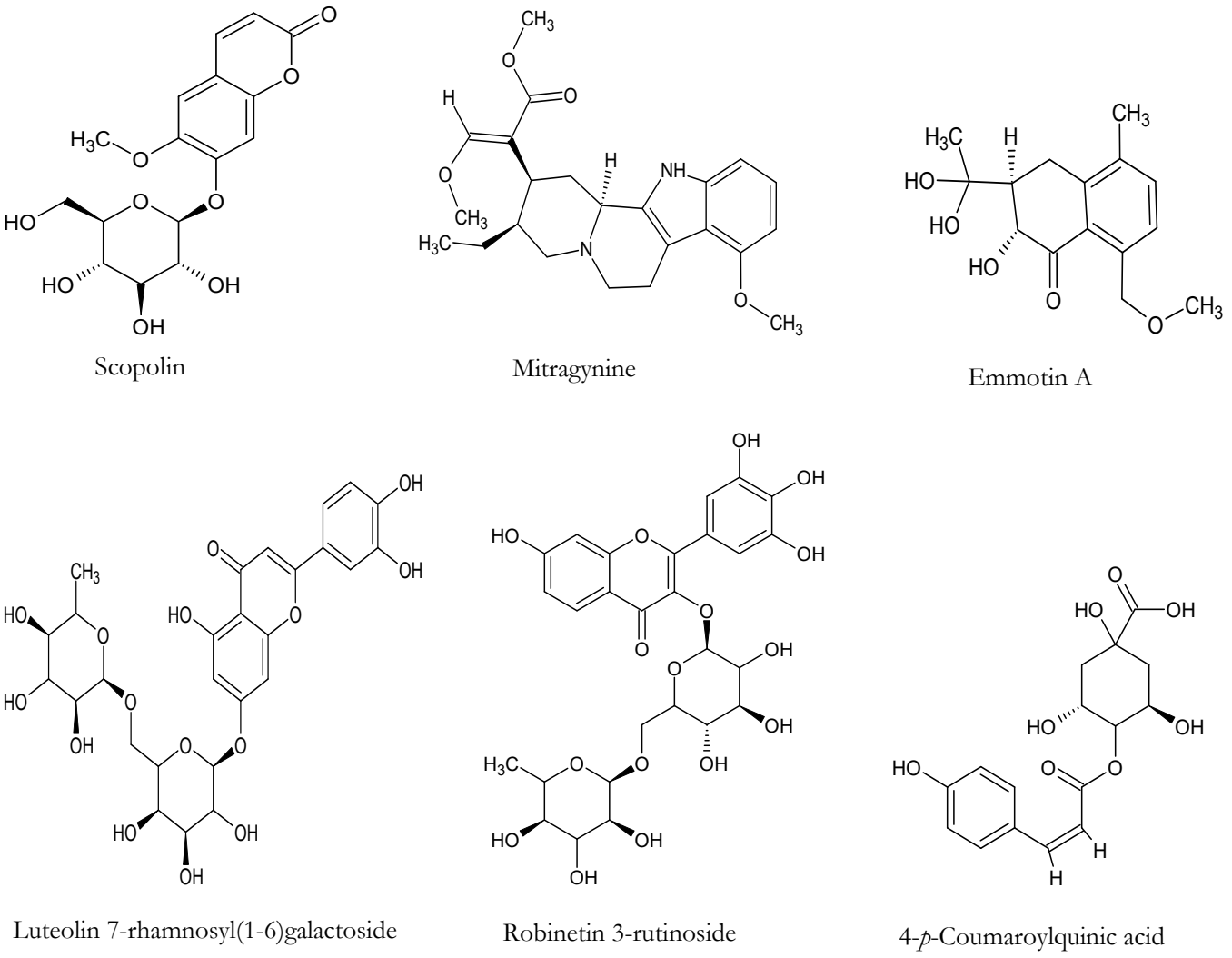

Figure 3: Chemical structures of some of the identified compounds of *M. speciosa* leaf 100%M extract

In silico Molecular Docking Analysis

The putative compounds identified through Q-ToF-LCMS analysis were subjected to molecular docking against two proteins (PDB ID: 3A4A and 4N8D), along with their respective native ligands and standard inhibitors. For PDB ID: 3A4A, the native ligand and the standard drug acarbose showed binding energies of -5.9 kcal/mol and -7.9 kcal/mol, respectively. The control docking of the native ligand yielded an RMSD value of 0.7, confirming the reliability of the docking protocol. Among the 13 compounds analyzed (Table 2), 6-hydroxyluteoin-7-(6'''-*p*-coumarylsophoroside) showed the strongest binding affinity (-11.9 kcal/mol), followed by apigenin 7-(2''-*E*-*p*-coumaroylglucoside) (-11.6 kcal/mol), luteolin 7-rhamnosyl(1-6)galactoside (-10.9 kcal/mol), robinetin 3-rutinoside (-10.0 kcal/mol), and 5,6,7,3',4'-pentahydroxy-8-methoxyflavone 7-apioside (-9.6 kcal/mol). The weakest binding affinity was observed for emmotin A (-7.2 kcal/mol); however, this value was still stronger than that of the native ligand and comparable to the standard acarbose. The binding interactions of 6-hydroxyluteoin-7-(6'''-*p*-coumarylsophoroside), apigenin 7-(2''-*E*-*p*-coumaroylglucoside), luteolin 7-rhamnosyl(1-6)galactoside, scopolin, and emmotin A, along with the native ligand and standard, against PDB ID: 3A4A are illustrated in Figure 4.

Table 2. The binding interactions along with the bond lengths of identified compounds of *M. speciosa* leaf 100%M extract against 3A4A

SI NO	Ligands	Binding affinity (kcal/mol)	Molecular Interactions	
			Hydrogen bond with bond distance (Å)	**Extra interactions with bond distance (Å)**
1.	*cis*-5-Caffeoylquinic acid	-8.4	SER 241; 2.47; ASP 242: 1.88; HIS 2.80: 2.36; THR 310: 2.91; SER 311: 2.30; PRO312: 2.09	TYR 158: 4.10; LYS 156: 5.34
2.	Scopolin	-8.5	SER 157: 2.30	HIS 280: 4.54; TYR 158: 3.73
3.	Apigenin 7-(2''-*E*-*p*-coumaroylglucoside)	-11.6	THR 310: 3.11; ASN 415: 2.24; HIS 112: 2.30; ASP 215: 3.09	VAL 216: 5.03; TYR 72: 5.79; PHE 178: 4.05; ARG 442: 4.31; ASP 307: 4.01; ARG 315: 5.39; HIS 280: 5.61
4.	4-*p*-Coumaroylquinic acid	-8.8	SER 241: 2.12; ASP 242: 2.09	TYR 158: 3.82; ARG 315: 3.78
5.	Epifisetinidol-4alpha-ol	-8.7	TYR 158: 2.47; ASP 215: 2.53; GLU 277: 2.16	VAL 216: 5.50; ASP 352: 4.57; ARG 442: 3.58; ARG 315: 5.35
6.	Robinetin 3-rutinoside	-10.0	ASN 415: 2.67; LEU 313: 2.34; PRO 312: 2.63 & 2.35; ASP 242; 2.52	-
7.	Kaempferol 3-(2''-(*Z*)-*p*-coumaryl-6''-(*E*)-*p*-coumarylglucoside)	-9.1	ASP 215: 2.91; GLU 411: 2.74 & 2.88; TYR 158: 2.51; LYS 156: 2.69; THR 310: 3.04; SER 311; 2.98; ARG 315: 2.32 & 3.08; ASP 242; 2.33	ASP 307: 4.65 & 3.38; ASP 242: 3.40; PRO 312: 3.89; TYR 158: 5.14; ASP 352; 4.46; VAL 216: 5.17; ASP 352; 4.46
8.	5,6,7,3',4'-Pentahydroxy-8-methoxyflavone 7-apioside	-9.6	ARG 442: 2.45; GLU 277: 2.22; HIS 280: 2.57; ASP 307: 2.65; PRO 312: 2.43; ARG 315: 2.23; LYS 156: 2.92	LEU 313: 3.44; ARG 315: 5.13 & 3.89
9.	Luteolin 7-rhamnosyl(1->6)galactoside	-10.9	PRO 312: 3.20; HIS 280: 3.00; THR 310: 1.78 & 3.02; ASP 307: 3.30 & 3.40; ARG 315: 2.71 & 2.30; ASP 69: 3.24; ASP 215: 3.05	ASP 215: 4.20; VAL 216: 5.09; GLU 277: 4.55; TYR 72: 5.72; PHE 303: 5.29 & 5.23
10.	6-Hydroxyluteoin-7-(6'''-*p*-coumarylsophoroside)	-11.9	ASP 69: 3.24; ASP 215: 3.05; ASP 307: 3.40 & 3.30; ARG 315: 2.71; PRO 312: 3.20; THR 310: 1.78 & 3.02; HIS 280: 3.09	TYR 72: 5.72; ASP 215: 4.20; VAL 216: 5.09; GLU 277: 4.55; PHE 303: 5.29 & 5.23; SER 240: 3.24
11.	Methyl reserpate	-9.4	PRO 312: 2.33; ARG 442: 2.48	PHE 178: 4.62; GLU 411: 4.47 & 4.73; TYR 158: 5.10
12.	Mitragynine	-8.0	HIS 280: 2.63; ARG 442: 2.83	PHE 303: 4.46 & 5.58
13.	Emmotin A	-7.2	ARG 315: 2.45	ARG 315: 4.28
Controls	Native Ligand	-5.9	GLU 277: 2.41 & 2.85; ASP 215: 2.62 & 3.10; HIS 351: 1.95; ARG 442: 1.85; ASP 69: 1.86	-
	Standard (acarbose)	-7.9	ASP 352: 2.79; GLU 277: 2.32; GLU 411: 2.66; HIS 280: 2.41; PRO 312: 1.74; TYR 158; 2.45	-

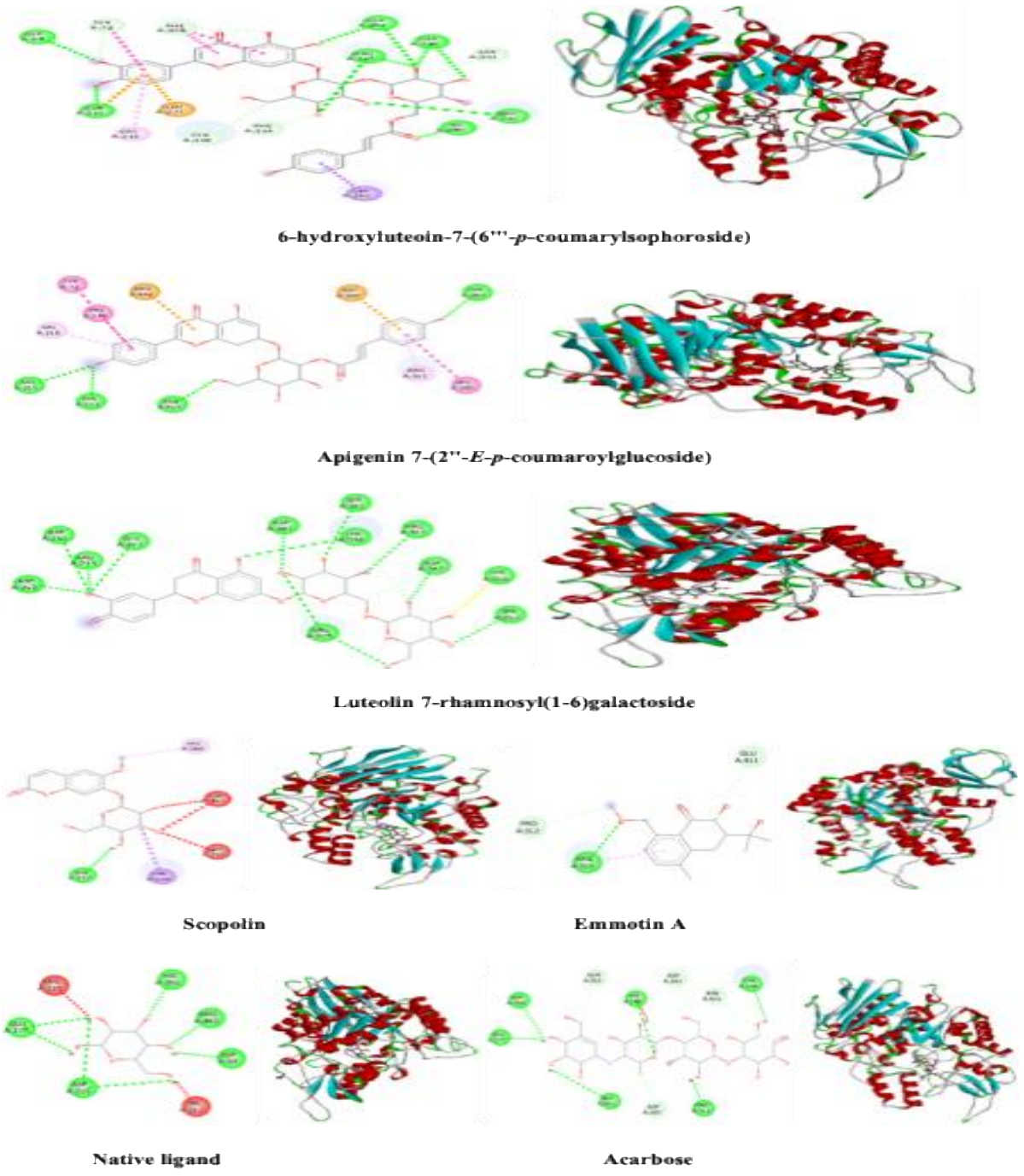

Figure 4: The binding interactions 6-hydroxyluteoin-7-(6'''-*p*-coumarylsophoroside), apigenin 7-(2''-*E*-*p*-coumaroylglucoside), luteolin 7-rhamnosyl(1-6)galactoside, scopolin, and emmotin A, along with the native ligand and standard against PDB ID: 3A4A

The compounds, along with the native ligand and standard inhibitor, exhibited diverse binding interactions with protein 3A4A. The native ligand interacted with the protein through conventional hydrogen bonds involving amino acid residues GLU 277, ASP 215, HIS 351, ARG 442, PRO 312, and ASP 69. For 6-hydroxyluteoin-7-(6'''-*p*-coumarylsophoroside), multiple amino acids contributed to hydrogen bonding and other non-covalent interactions. Specifically, ASP 69, ASP 215, ASP 307, ARG 315, PRO 312, THR 310, and HIS 280 were involved in conventional

hydrogen bonds. In the case of apigenin 7-(2''-*E*-*p*-coumaroylglucoside), hydrogen bonds were formed with THR 310, ASN 415, HIS 112, and ASP 215. Emmotin A, which showed the lowest binding energy among the analyzed compounds, interacted with ARG 315 through both hydrogen bonding and additional non-covalent interactions. The standard inhibitor (acarbose) formed hydrogen bonds with ASP 352, GLU 277, GLU 411, HIS 280, PRO 312, and TYR 158.

Conversely, for PDB ID: 4N8D, the native ligand and standard inhibitor sitagliptin showed binding energies of -8.4 kcal/mol and -9.4 kcal/mol, respectively. The control docking of the native ligand produced an RMSD value of 1.57, validating the docking protocol. Among the 13 compounds analyzed (Table 3), luteolin 7-rhamnosyl(1-6)galactoside demonstrated the strongest binding affinity (-11.2 kcal/mol), followed by 6-hydroxyluteoin-7-(6'''-*p*-coumarylsophoroside) (-11.0 kcal/mol), kaempferol 3-(2''-(*Z*)-*p*-coumaryl-6''-(*E*)-*p*-coumarylglucoside) (-10.8 kcal/mol), robinetin 3-rutinoside (-10.3 kcal/mol), and apigenin 7-(2''-*E*-*p*-coumaroylglucoside) (-10.1 kcal/mol). The weakest binding affinity was observed for emmotin A (-7.9 kcal/mol), although this value was still stronger than that of the native ligand. The binding interactions of luteolin 7-rhamnosyl(1-6)galactoside, 6-hydroxyluteoin-7-(6'''-*p*-coumarylsophoroside), kaempferol 3-(2''-(*Z*)-*p*-coumaryl-6''-(*E*)-*p*-coumarylglucoside), scopolin, and emmotin A, along with the native ligand and standard, against PDB ID: 4N8D are shown in Figure 5.

Table 3. The binding interactions, along with the bond lengths of identified compounds of *M. speciosa* leaf 100%M extract against 4N8D

SI NO	Ligands	Binding affinity(kcal/mol)	Molecular Interactions	
			Hydrogen bond with bond distance (Å)	**Extra bond interactions with bond distance (Å)**
1.	*cis*-5-Caffeoylquinic acid	-8.4	SER 630: 2.25; GLU 205: 2.11; HIS 740: 2.58; TRP 629: 2.26; VAL 546: 2.28	-
2.	Scopolin	-8.2	GLU 206: 2.88; ARG 125: 2.34; GLU 205: 2.80	GLU 205: 4.60; TYR 666: 4.99 & 5.64; TYR 662: 4.63
3.	Apigenin 7-(2''-*E*-*p*-coumaroylglucoside)	-10.1	VAL 546: 3.26; ASP 545: 3.35; LYS 554: 2.37; SER 630: 3.02; TYR 631: 2.68; ARG 358: 2.70 & 2.86	TYR 666: 4.11; TYR 547: 4.58 & 4.29
4.	4-*p*-Coumaroylquinic acid	-8.5	ARG 125: 2.93	TYR 547: 4.31
5.	Epifisetinidol-4alpha-ol	-8.1	LYS 554: 2.15; TRP 629: 2.48	TYR 547: 4.18; TYR 666: 5.82
6.	Robinetin 3-rutinoside	-10.3	VAL 546: 2.67; LYS 554: 1.91 & 2.60; TRP 629: 2.12; ARG 125: 2.54; SER 630: 2.47; HIS 740: 2.83;	PHE 357: 4.42 & 5.72; TYR 666: 5.10; TYR 662: 5.07

			ASN 710: 2.28; GLU 206: 2.77; ARG 358: 2.04	
7.	Kaempferol 3-(2''-(*Z*)-*p*-coumaryl-6''-(*E*)-*p*-coumarylglucoside)	-10.8	ARG 358: 2.58; GLU 206: 3.25; ARG 669: 2.84; GLU 205: 3.20; ARG 125: 2.62 & 2.52; LYS 554: 2.11	TRP 629: 3.81; PHE 357: 3.99
8.	5,6,7,3',4'-Pentahydroxy-8-methoxyflavone 7-apioside	-9.2	VAL 546: 2.86; TRP 629: 2.86; GLU 205: 2.14; GLU 206: 2.38; ARG 358: 2.42 & 2.35; SER 209: 2.02	PHE 357: 3.74; TYR 666: 5.48; ARG 125: 4.70; TYR 547: 4.82 & 3.69
9.	Luteolin 7-rhamnosyl(1->6)galactoside	-11.2	SER 209: 2.72; ARG 358: 1.82; TYR 631: 2.28; HIS 740: 3.37; LYS 122: 3.05 & 2.04; ASP 739: 3.30; GLU 205: 2.99; ARG 125: 2.87, 2.55 & 2.71	ARG 125: 4.62
10.	6-Hydroxyluteoin-7-(6'''-*p*-coumarylsophoroside)	-11.0	TYR 752: 2.83; ARG 358: 2.74; ARG 125: 2.20; SER 209: 2.53; HIS 740: 3.10; SER 630: 2.06; GLU 205: 3.59; GLU 206: 3.00; TYR 662: 3.28; TYR 631: 2.15; VAL 546: 3.37; LYS 554: 2.30; TRP 629: 2.91	TYR 666: 5.86; TRP 629: 3.87; ARG 125: 4.45
11.	Methyl reserpate	-8.6	ARG 358: 2.57; GLU 206: 1.95	-
12.	Mitragynine	-8.0	TYR 547: 2.99; TRP 629: 2.78; TYR 631: 2.52; TRP 629: 2.78	TYR 547: 3.88 & 4.41; LYS 554: 5.28
13.	Emmotin A	-7.9	SER 630: 1.99; TRP 629: 2.51	TRP 629: 3.99
Controls	Native Ligand	-8.4	TYR 662: 1.79	PHE 357: 4.50; SER 630: 4.96; TYR 666: 4.96; TYR 662: 4.44; GLU 206: 2.90; GLU 205: 2.03; ASP 663: 4.84
	Standard (sitagliptin)	-9.4	TYR 662: 2.79; HIS 740: 2.58	TYR 662: 4.04; VAL 656: 5.02; TYR 666: 4.66; LYS 554: 4.81; TRP 629: 3.65; ASP 545: 3.32

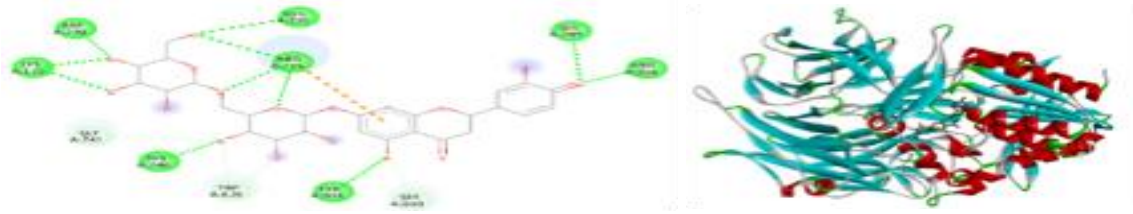

Luteolin 7-rhamnosyl(1-6)galactoside

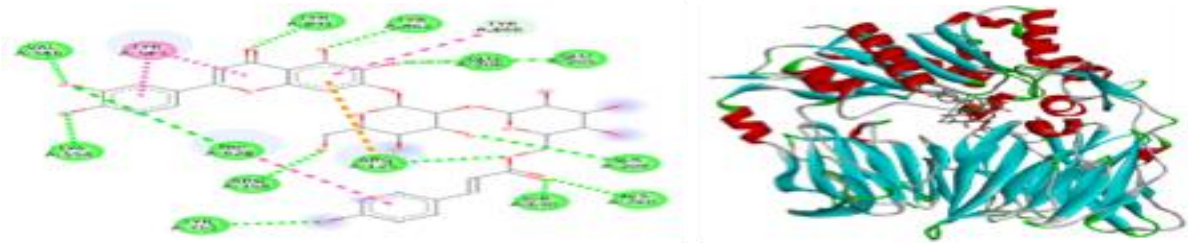

6-hydroxyluteoin-7-(6'''-*p*-coumarylsophoroside)

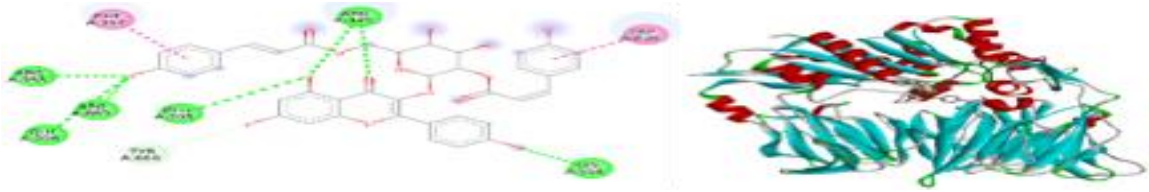

Kaempferol 3-(2''-(*Z*)-*p*-coumaryl-6''-(*E*)-*p*-coumarylglucoside)

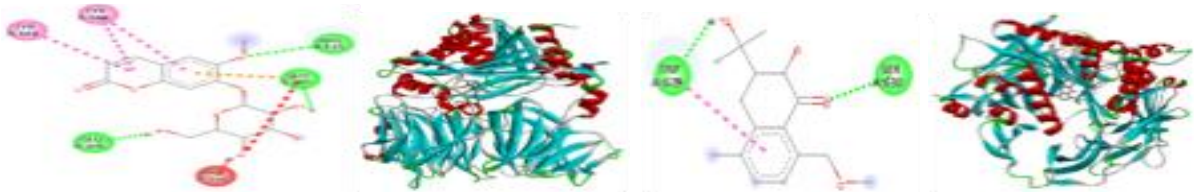

Scopolin Emmotin A

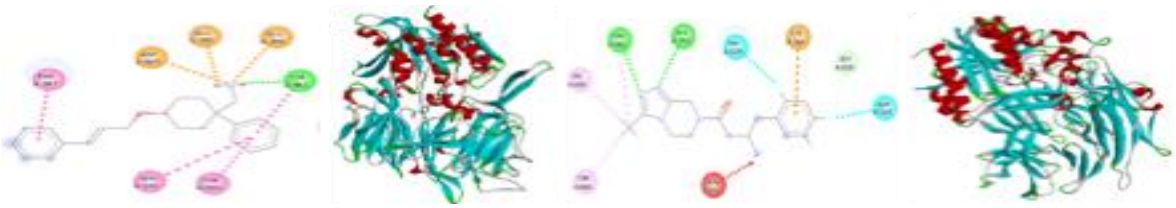

Native ligand Sitagliptin

Figure 5: The binding interactions of luteolin 7-rhamnosyl(1-6)galactoside, 6-hydroxyluteoin-7-(6'''-*p*-coumarylsophoroside), kaempferol 3-(2''-(*Z*)-*p*-coumaryl-6''-(*E*)-*p*-coumarylglucoside), scopolin, and emmotin A, along with the native ligand and standard against PDB ID: 4N8D

Against the protein target 4N8D, the compounds, along with the native ligand and standard inhibitor, exhibited distinct binding interactions. The native ligand formed a hydrogen bond with amino acid TYR 662, and additional non-covalent interactions with amino acid residues PHE 357, SER 630, TYR 666, TYR 662, GLU 206, GLU 205, and ASP 663. For luteolin 7-rhamnosyl(1->6)galactoside, hydrogen bonds were established with SER 209, ARG 358, TYR 631, HIS 740, LYS 122, ASP 739, GLU 205, and ARG 125. Scopolin (-8.2 kcal/mol) interacted through hydrogen bonds with GLU 206, ARG 125, and GLU 205. Emmotin A (-7.9 kcal/mol), which showed the weakest binding affinity among the analyzed compounds, formed hydrogen bonds with SER 630, and TRP 629. The standard inhibitor, sitagliptin exhibited hydrogen bonding interactions with TYR 662, and HIS 740, consistent with its

strong binding affinity.

Physico-Chemical and Pharmacokinetics Properties

All thirteen compounds identified from the *M. speciosa* leaf 100%M extract through Q-ToF LCMS analysis were further evaluated for their physicochemical and pharmacokinetic profiles to understand their drug likenesses and toxicity profiles (Table 5).

Table 5. The physicochemical and pharmacokinetic parameters of compounds identified from *M. speciosa* leaf 100%M extract

Compound	Physicochemical						Pharmacokinetic & Toxicity				
	HA	HD	MW	Log P	V	DL	IA	CR	HT	AM	ROAT
Epifisetinidol-4alpha-ol	6	5	290	-0.02	0	Yes	65.56	0.003	No	Yes	2.45
6-hydroxyluteoin-7-(6'''-*p*-coumarylsophoroside)	19	11	773	-3.64	3	No	17.24	-0.44	No	No	2.49
Luteolin 7-rhamnosyl(1-6)galactoside	15	9	595	-3.43	3	No	27.78	0.25	No	Yes	2.73
Mitragynine	5	1	399	2.02	0	Yes	92.97	0.86	Yes	No	3.16
Robinetin 3-rutinoside	16	10	611	-3.89	3	No	20.60	-0.38	No	No	2.50
1,4-di-o-caffeoylquinic acid	12	7	517	-0.35	3	No	16.36	-0.06	No	No	2.54
5,6,7,3',4'-pentahydroxy-8-methoxyflavone 7-apioside	12	7	464	-2.32	2	No	41.38	0.44	No	No	2.61
Apigenin 7-(2''-*E*-*p*-coumaroylglucoside	12	6	579	-0.56	3	No	47.64	0.04	No	No	2.62
Emmotin A	4	2	278	0.96	0	Yes	95.02	1.05	No	No	2.04
Methyl reserpate	6	2	415	1.30	0	Yes	93.52	48.12	Yes	No	2.93
Scopolin	9	4	354	-1.23	0	Yes	48.12	0.72	No	No	2.39
Kaempferol 3-(2''-(*Z*)-*p*-coumaryl-6''-(*E*)-*p*-coumarylglucoside)	15	7	741	3.6953	3	No	63.18	-0.38	No	No	2.51
4-*p*-coumaroylquinic acid	7	5	338	-0.35	0	yes	27.58	0.44	No	No	1.77

Note: HA: hydrogen bond acceptor; HD: hydrogen bond donor; MW: molecular weight, gram/mole; Log P: predicted octanol/water partition coefficient; DL: drug likeness; V: number of violations to Lipinski's rule; IA: intestinal absorption, %; CR: clearance; %; HT: hepatotoxicity; AM: AMES toxicity; ROAT: rat oral acute toxicity, mol/kg

DISCUSSION

The 100%M extract derived from *M. speciosa* leaves using the maceration extraction technique yielded a substantial amount of 30.17%, indicating efficient extraction of bioactive compounds from the source material. This relatively high yield suggests that the extraction method employed was suitable for recovering a broad spectrum of phytochemicals, which is essential for downstream pharmacological or nutraceutical applications (Ahmed et al., 2025).

The Q-ToF-LCMS analysis revealed a diverse array of phytochemical constituents, identified through both positive and negative ionization modes. This dual-mode approach enhances the sensitivity and coverage of compound detection, as certain phytoconstituents ionize more effectively in one mode than the other. Among the identified compounds, several phenolic and flavonoid compounds were detected, including *cis*-5-caffeoylquinic acid, 4-*p*-coumaroylquinic acid, epifisetinidol-4alpha-ol, robinetin 3-rutinoside, kaempferol 3-(2''-(*Z*)-*p*-coumaryl-6''-(*E*)-*p*-coumarylglucoside), 5,6,7,3',4'-pentahydroxy-8-methoxyflavone 7-apioside, luteolin 7-rhamnosyl(1->6)galactoside, 6-hydroxyluteoin-7-(6'''-*p*-coumarylsophoroside), and apigenin 7-(2''-*E*-*p*-coumaroylglucoside). Earlier works have revealed that flavonoids are responsible for various pharmacological activities, including anti-diabetic effects. For instance, rutin has been shown to retard carbohydrate absorption by obstructing the α-glucosidase enzyme activity, kaempferol can increase glucose uptake, and luteolin is capable of inhibiting lipid synthesis (Praparatana et al., 2022). Moreover, 4-*p*-coumaroylquinic acid has been reported to exert antidiabetic activity in albino Wistar rats (Amalan et al., 2016). These findings suggest that the phenolic and flavonoid compounds identified in kratom leaf extract may contribute to its antidiabetic potential. Beyond these, mitragynine has already been documented to possess antidiabetic properties (Limcharoen et al., 2022). Furthermore**,** scopolin (scopoletin-7-O-β-*D*-glucopyranoside) is a glycoside of scopoletin, has also been linked to antidiabetic activity **(**Jang et al., 2020**).**

The tentative phytoconstituents detected via Q-ToF-LCMS analysis were subjected to the molecular docking against two diabetes linked proteins (PDB ID: 3A4A and 4N8D), along with their respective native ligands and standard inhibitors. Compared to the native ligands and standard inhibitors, the compounds identified from the 100%M extract showed strong binding affinities against both diabetes-associated protein targets. Alpha-glucosidase inhibitors, such as acarbose are the drugs that retard carbohydrate absorption from the small intestine by competitively inhibiting the enzymes accountable for converting intricate carbohydrates into simple carbohydrates which are easily absorbed. By delaying carbohydrate absorption, these drugs effectively reduce postprandial blood glucose concentrations (Akmal et al., 2024). Several of the identified compounds showed binding affinities and interaction profiles that were not only comparable to, but in some cases stronger than, acarbose against the alpha-glucosidase enzyme (3A4A). These findings provide a promising baseline for the development of novel alpha-glucosidase inhibitors.

Similarly, DPP-4 inhibitors such as sitagliptin exert their antidiabetic effects through modulation of incretin hormones. Incretins are secreted within minutes of food intake but are rapidly degraded by the DPP-4 enzyme. By inhibiting DPP-4, these drugs prolong incretin activity, thereby enhancing insulin secretion and reducing postprandial and fasting hyperglycemia. Beyond their antihyperglycemic effects, DPP-4 inhibitors have also been reported to exert antihypertensive, anti-inflammatory, antiapoptotic, and immunomodulatory effects on the cardiovascular and renal systems, independent of the incretin pathway (Kasina, & Baradhi, 2019). The identified compounds from the 100%M extract displayed binding affinities and interactions that were comparable to, and in some cases stronger than, those of the native ligand and sitagliptin, suggesting their potential as promising scaffolds for the development of new DPP-4 inhibitors.

The assessment of physicochemical and pharmacokinetic parameters is essential to evaluate the potential of bioactive compounds as lead candidates for the development of new drug products. Accordingly, all thirteen compounds identified from the 100%M extract were further evaluated for their physicochemical and pharmacokinetic profiles. The assessment revealed that out of the 13 compounds, epifisetinidol-4alpha-ol, mitragynine, emmotin A, methyl reserpate, scopolin, and 4-*p*-coumaroylquinic acid showed drug likeness. Among these, epifisetinidol-4alpha-ol, mitragynine, and methyl reserpate were predicted to possess either AMES mutagenicity or hepatotoxicity. In contrast, 4-*p*-coumaroylquinic acid, scopolin, and emmotin A showed no predicted toxicity, with intestinal absorption values of low (27.577%), medium (48.119%) and high (95.021%), respectively. Advances in drug design and formulation strategies may help overcome limitations such as poor absorption or toxicity. Approaches including particle size reduction, increased surface area, and prodrug formation have been successfully employed to enhance bioavailability and reduce adverse effects (Alagga et al.,

2025). Although the other flavonoid compounds showed strong binding affinities against both protein targets, their high molecular weight and hydrophilic nature limited their drug-likeness. Structural optimization, such as the introduction of small hydrophobic groups, could improve their pharmacokinetic properties and enhance their potential as drug candidates (Sarian et al., 2017).

CONCLUSION

The global incidence of diabetes is escalating at an alarming pace, creating an urgent demand for novel antidiabetic therapies that can overcome the limitations, tolerance, and side effects associated with existing drugs. Natural products remain a valuable reservoir for drug discovery, and in this context, kratom leaves represent a promising source of bioactive compounds. The present study establishes a baseline for future research aimed at isolating and developing antidiabetic agents from kratom leaves. Among the identified compounds, 4-*p*-coumaroylquinic acid, scopolin, and emmotin A emerged as particularly noteworthy, demonstrating favourable binding affinities, pharmacokinetic properties, and safety profiles. These findings highlight their potential as lead compounds for the development of novel antidiabetic drugs. Overall, the findings support the potential of the 100%M extract as a rich source of bioactive compounds. Future studies should focus on isolating individual constituents, evaluating their pharmacological effects, and exploring synergistic interactions that may enhance therapeutic efficacy.

ACKNOWLEDGEMENT

This study was partially supported by the CRIGS UKM-IIUM-UiTM-UPM Research Collaboration Grant 2024 (C-RIGS24-017-0023), under the Research Management Centre, International Islamic University Malaysia (IIUM). The authors gratefully acknowledge the financial support provided by Regal Malay Capital Berhad, Malaysia (SPP22-137-0137), and the CPS Sejahtera Award, IIUM. We also extend our sincere appreciation to the Kulliyyah of Pharmacy, IIUM, for providing the research facilities necessary to complete this work.

AUTHORS CONTRIBUTIONS

Conceptualization, Q.U.A.; M.M.A.K.K.; T.B.; methodology, T.B.; Q.U.A.; resources, Q.U.A.; M.H.A.; data curation, T.B.; M.S.R.; S.A.A.S.; writing-original draft preparation, T.B.; writing-review and editing, Q.U.A.; M.M.A.K.K.; M.N.S.; visualization, Q.U.A.; A.B.M.H.U.; M.N.S.; supervision, Q.U.A. All authors have read and agreed to the published version of the manuscript.

CONFLICT OF INTEREST

The authors declare that they have no conflicts of interest.

DATA AVAILABILITY

Data will be made available on reasonable request.

FUNDING

No direct funding was received to assist with the preparation of this manuscript.

ETHICAL APPROVAL

Not applicable.

REFERENCES

Ahmed, Q. U., Atirah Ali, S. N. A., Abdul Jalil, N. N. S., Uddin, A. H., Rofiee, M. S., Ali Shah, S. A., Salleh, M. Z., Abbas, S. A., Ahmed, M. Z., Sarker, M. Z. I. & Mia, M. A. R. (2025). Unveiling the anti-diabetic effects of *Garcinia hombroniana* fruit pericarp and leaf: *in vitro* radical scavenging, alpha-glucosidase inhibition, pharmacokinetics, and *in silico* molecular docking of Q-TOF-LCMS identified compounds. *Natural Product Research*, 1-12. https://doi.org/10.1080/14786419.2025.2534861

Akmal, M., Patel, P., & Wadhwa, R. (2024). *Alpha glucosidase inhibitors.* StatPearls Publishing. https://www.ncbi.nlm.nih.gov/books/NBK557848/

Alagga, A. A., Pellegrini, M. V., & Gupta, V. (2024). *Drug Absorption.* StatPearls Publishing. https://www.ncbi.nlm.nih.gov/books/NBK557405/.

Amalan, V., Vijayakumar, N., Indumathi, D., & Ramakrishnan, A. (2016). Antidiabetic and antihyperlipidemic activity of p-coumaric acid in diabetic rats, role of pancreatic GLUT 2: *In vivo* approach. *Biomedicine & Pharmacotherapy*, *84*, 230-236. https://doi.org/10.1016/j.biopha.2016.09.039

Ananda, Z. K, Begum, T., Ahda, M., Rofiee, M. S., Shah, S. A. A., Salleh, M. Z., Almutairi, B.O., Azmi, S. N. H., Sah, P., Wardani, A. K., Khatib, A., Abbas, S. A., Mia, M. A. R., Ahmed, Q. U. (2025). Comparative evaluation of phytochemical screening, *in vitro* antioxidant & alpha-glucosidase inhibitory properties of *Ceiba pentandra* & *Basella rubra* leaf extracts: Identification of active principles by Q-TOFLCMS, ADMET prediction &

molecular docking approach. *Journal of King Saud University - Science*, *37*(1), 162024. https://doi.org/10.25259/JKSUS_16_2024

Begum, T., Arzmi, M. H., Khatib, A., Uddin, A. H., Aisyah Abdullah, M., Rullah, K., So'ad, S. Z. M., Haspi, N. F. Z., Sarian, M. N., Parveen, H., Mukhtar, S., Ahmed, Q. U. (2025a). A review on *Mitragyna speciosa* (Rubiaceae) as a prominent medicinal plant based on ethnobotany, phytochemistry and pharmacological activities. *Natural Product Res*earch, *39*, 1636-1652. https://doi.org/10.1080/14786419.2024.2371564

Begum, T., Ahmed, Q. U., Arzmi, M. H., Uddin, A. H., Khatib, A., Mohamad, S. N. A. S., Nasarudin, S. N. I. S., Abbas, S. A., Abd Aziz, Z. H. (2025b). Phytochemical screening and evaluation of *in vitro* antioxidant, antibacterial and antibiofilm activities of *Mitragyna speciosa* leaf extract. *Malaysian Journal of Chemistry*, *27*(5), 80-94.

Fadly, D. (2025). *Blood glucose response to kratom tea (Mitragyna speciosa Korth.).* BIO Web of Conferences (Vol. 153, p. 03015). EDP Sciences. https://doi.org/10.1051/bioconf/202515303015

Hossain, M. U., Hossain, M. S., Dey, S., Naimur Rahman, A. B. Z., Chowdhury, Z. M., Bhattacharjee, A., Ahammad, I., Islam, M. N., Moniruzzaman, M., Hosen, M. B., Ahmed, I., Das, K. C., Keya, C. A.,& Salimullah, M. (2023). *In vivo* and *in silico* experiment on *Mitragyna speciosa* offers new insight of antidiabetic potentials. *bioRxiv*, *2023*, 11. https://doi.org/10.1101/2023.11.08.566341

International Diabetes Federation. (2025). *IDF Diabetes Atlas* (11th ed.). IDF. https://diabetesatlas.org/resources/idf-diabetes-atlas-2025/

Jang, J. H., Park, J. E., & Han, J. S. (2020). Scopoletin increases glucose uptake through activation of PI3K and AMPK signaling pathway and improves insulin sensitivity in 3T3-L1 cells. *Nutrition Research*, *74*, 52-61. https://doi.org/10.1016/j.nutres.2019.12.003

Kasina, S. V. S. K., & Baradhi, K. M. (2019). *Dipeptidyl peptidase iv (DPP IV) inhibitors.* StatPearls. https://www.ncbi.nlm.nih.gov/books/NBK542331/

Limcharoen, T., Pouyfung, P., Ngamdokmai, N., Prasopthum, A., Ahmad, A. R., Wisdawati, W., Prugsakij, W., & Warinhomhoun, S. (2022). Inhibition of α glucosidase and pancreatic lipase properties of *Mitragyna speciosa* (Korth.) Havil. (kratom) leaves. *Nutrients*, *14*(19), 3909. https://doi.org/10.3390/nu14193909

Mia, M. A. R., Ahmed, Q. U., Ferdosh, S., Helaluddin, A. B. M., Awal, M. S., Sarian, M. N., Sarker, M. Z. I., & Zakaria, Z. A. (2022). *In vitro, in silico* and network pharmacology mechanistic approach to investigate the α-glucosidase inhibitors identified by Q-ToF-LCMS from *Phaleria macrocarpa* fruit subcritical CO2 extract. *Metabolites*, *12*(12), 1267. https://doi.org/10.3390/metabo12121267

Pollack, M. F., Purayidathil, F. W., Bolge, S. C., & Williams, S. A. (2010). Patient-reported tolerability issues with oral antidiabetic agents: associations with adherence; treatment satisfaction and health-related quality of life. *Diabetes research and clinical practice*, *87*(2), 204-210. https://doi.org/ 10.1016/j.diabres.2009.11.023

Praparatana, R., Maliyam, P., Barrows, L. R., & Puttarak, P. (2022). Flavonoids and Phenols, the Potential Anti-Diabetic Compounds from *Bauhinia strychnifolia* Craib. Stem. *Molecules*, *27*(8), 2393. https://doi.org/10.3390/molecules27082393

Sarian, M. N., Ahmed, Q. U., Mat So'ad S. Z., Alhassan, A. M., Murugesu, S., Perumal, V., Perumal, V., Mohamad, S. N. A. S., Khatib, A., & Latip, J. (2017). Antioxidant and antidiabetic effects of flavonoids: A structure-activity relationship based study. *BioMed research International*, *2017*(1), 8386065. https://doi.org/10.1155/2017/8386065

Trott, O., & Olson, A. J. (2010) AutoDockVina: Improving the speed and accuracy of docking with a new scoring function, efficient optimization, and multithreading. *Journal of Computational Chemistry*, *31*, 455-61. https://doi.org/10.1002/jcc.21334

Zhang, P., Wei, W., Zhang, X., Wen, C., Ovatlarnporn, C., & Olatunji, O. J. (2023). Antidiabetic and antioxidant activities of *Mitragyna speciosa* (kratom) leaf extract in type 2 diabetic rats. *Biomedicine & Pharmacotherapy*, *162*, 114689. https://doi.org/10.1016/j.biopha.2023.114689